

Lewis acidity of group 14 elements toward intramolecular sulfur in ortho-aryl-thioanisoles¹

Teresita Munguia, Ioana S. Pavel, Ramesh N. Kapoor, Francisco Cervantes-Lee, László Párkányi, and Keith H. Pannell

Abstract: The series of compounds (*o*-CH₃SC₆H₄)CH₂EPh₃ (E = Si (1), Ge (2), Sn (3), and Pb (4)) have been synthesized and characterized by NMR spectroscopy and by single crystal X-ray diffraction. Compounds 1 and 2 are isostructural with a triclinic crystal system and *P*-1 space group; however, morphotropic steps occur between Ge and Sn, and Sn and Pb. While the E-S distances in 1 and 2 are 3.985 and 3.974 Å, respectively, ~100% of the sum of the respective van der Waals (vdW) radii, there is a notable distortion from tetrahedral geometry about E. Compound 3 is also triclinic with *P*-1 symmetry, but has two molecules in the unit cell that demonstrate a distorted tetrahedral geometry and intramolecular Sn-S distances of 3.699 and 3.829 Å, 88% and 91% of the sum of the vdW radii. Compound 4 has a Pb-S distance of 3.593 Å (91% of Σ vdW radii). The structure of the Grignard coupling product [*o*-(SCH₃)C₆H₄CH₂]₂ is also reported.

Key words: intramolecular self-assembly, silicon, germanium, tin, lead, sulfur.

Résumé : On a réalisé la synthèse d'une série de composés de formule (*o*-CH₃SC₆H₄)CH₂EPh₃ dans lesquels E = Si (1), Ge (2), Sn (3) et Pb (4) et on les a caractérisés par spectroscopie RMN et par diffraction des rayons X par un cristal unique. Les composés 1 et 2 sont isostructuraux avec un système cristallin triclinique et un groupe d'espace *P*-1; toutefois, on note des différences morphotropes entre le Ge et le Sn ainsi qu'entre le Sn et le Pb. Alors que les distances E-S dans les composés 1 et 2 sont respectivement de 3,985 et 3,974 Å, environ 100 % de la somme des rayons respectifs de van der Waals, on note une distorsion notable par rapport à la géométrie tétraédrique autour de E. Le composé 3 est aussi triclinique avec une symétrie *P*-1, mais la maille cristalline comporte deux molécules ce qui démontre la présence d'une géométrie tétraédrique déformée alors que les distances intramoléculaires Sn-S de 3,699 et 3,829 Å correspondent respectivement à 88 % et 91 % de la somme des rayons de van der Waals. Dans le composé 4, la distance Pb-S est de 3,593 Å (91 % de la somme des rayons de van der Waals). On a aussi déterminé la structure du produit de couplage de Grignard [*o*-(SCH₃)C₆H₄CH₂]₂.

Mots clés : auto-assemblage intramoléculaire, silicium, germanium, étain, plomb, soufre.

[Traduit par la Rédaction]

Introduction

The system (*o*-CH₃SC₆H₄)CH₂EPh₃ (E = Si (1), Ge (2), Sn (3), and Pb (4)) offers the capacity to examine intramolecular sulfur-metal interactions via a five-membered ring involving the *ortho*-thiomethyl group S atom (Fig. 1), such that the varying Lewis acidities of the elements toward sulfur may be evaluated. Furthermore, this possible hyper-

valency could impact the potential morphotropic steps as originally described by Kitaigorodskii (1), and observed for simpler group 14 systems where only tetrahedral structures were possible. For example, the system Ph₄E (E = Si (2), Ge (3), Sn (4), Pb (5)) has been analyzed with respect to such structural variations, and more recent studies by Párkányi et al. (6) illustrated a morphotropic step occurring in the heteronuclear intra(inter)-group 14 bonding organometallic compounds (R₃EE'R₂). In these systems the packing coefficient, defined as:

$$\eta = \frac{ZV_m}{V}$$

where *Z* is the number of molecules in the unit cell, *V_m* is the volume of the molecule, and *V* is the unit cell volume, must be significantly decreased to change the packing motif and create a morphotropic step (6). Thus, 1–4 present an appealing series with which to study whether the size changes of the group 14 element would be sufficient to change the packing coefficient. Furthermore, would the potential intramolecular metal-sulfur interaction be adequate to distort the tetrahedral geometry about the metal center and further aid, or impede, the potential for a morphotropic step.

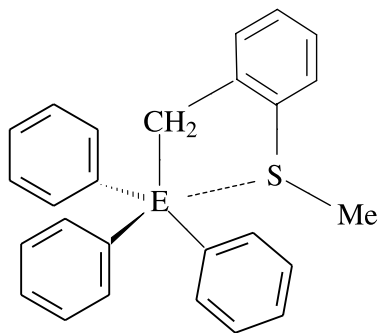
Received 12 March 2003. Published on the NRC Research Press Web site at <http://canjchem.nrc.ca> on 5 November 2003.

John: It has been one of my pleasures to get together with you periodically to talk, drink, and generally enjoy your company as well as your chemistry. Cheers, Keith.

T. Munguia, I.S. Pavel, R.N. Kapoor, F. Cervantes-Lee, and K.H. Pannell.² Department of Chemistry, University of Texas at El Paso, El Paso, Texas 79968-0513, U.S.A.
L. Párkányi. Central Research Institute of Chemistry, Hungarian Academy of Sciences, H-1525 Budapest, P.O. Box 17, Hungary.

¹This article is part of a Special Issue dedicated to Professor John Harrod.

²Corresponding author (e-mail: kpannell@utep.edu).

Fig. 1. Triphenyl group 14 derivatives of *o*-aryl thioanisole.

E = Si, Ge, Sn, Pb

Compounds in which systematic evaluations of the intramolecular interactions among group 14 organometallic compounds have been previously reported but were limited to investigations between tin and sulfur, as demonstrated by Wardell and co-workers (7), Tzschach and co-workers (8), and Dräger and co-workers (9) (Fig. 2).

Experimental section

General techniques

All syntheses were performed under a nitrogen atmosphere using standard Schlenk line techniques. Reagent grade tetrahydrofuran (THF) and hexanes were dried and distilled under nitrogen from a sodium benzophenone ketyl solution; benzene was dried and distilled from Na ribbon. Thionyl chloride was purchased from Fisher Scientific and purified by distillation; pyridine was purchased from E M Science and dried and distilled over KOH; Ph_3SiCl and Ph_3GeCl were purchased from Gelest; Ph_3SnCl , Ph_3PbCl , thiosalicylic acid, and dimethyl sulfate were purchased from Aldrich and were used as received. NMR spectra of all compounds were recorded on a Bruker 300 MHz spectrometer in CDCl_3 . Elemental analyses were performed by Galbraith Laboratories.

Syntheses of *o*-(methylthio)benzoic acid (10), *o*-(methylthio)benzyl alcohol (10, 11), and *o*-(methylthio)benzyl chloride (12) followed literature procedures. *o*-(Methylthio)benzoic acid, mp 165 °C (lit. (10) value 167–169 °C). ^1H NMR (CDCl_3) δ : 2.5 (3H, s, S-CH₃), 7.2–7.5 (4H, m, Ph), 8.1 (1H, d, COOH). ^{13}C NMR (CDCl_3) δ : 15.6 (S-CH₃), 123.5, 124.4, 125.5, 132.5, 133.3 (C_{ipso}), 144.4 (C_{ipso}), 171.5 (COOH). *o*-(Methylthio)benzyl alcohol, bp 156 °C/17 mmHg (1 mmHg = 133.322 Pa) (lit. (10) value 88 °C/0.001 mmHg (1 mmHg = 133.322 Pa)). ^1H NMR (CDCl_3) δ : 2.4 (3H, s, S-CH₃), 3.3 (1H, s, OH), 4.7 (2H, s, CH₂-OH), 7.2–7.4 (4H, m, Ph). ^{13}C NMR (CDCl_3) δ : 16.3 (S-CH₃), 63.2 (CH₂-OH), 125.7, 126.5, 128.0, 128.5, 136.8 (C_{ipso}), 139.3 (C_{ipso}). *o*-(Methylthio)benzyl chloride, bp 123 °C/9 mmHg (1 mmHg = 133.322 Pa) (lit. (12) value 75 to 76 °C/1 × 10⁻² mmHg (1 mmHg = 133.322 Pa)). ^1H NMR (CDCl_3) δ : 2.5 (3H, s, S-CH₃), 4.8 (2H, s, CH₂-Cl), 7.2–7.4 (4H, m, Ph). ^{13}C NMR (CDCl_3) δ : 16.7 (S-CH₃), 45.1 (CH₂-Cl), 126.0, 127.3, 129.9, 130.6, 136.0 (C_{ipso}), 139.1 (C_{ipso}).

The syntheses of the group 14 derivatives of *o*-(methylthio)benzyl chloride were accomplished as illustrated below for the silicon derivative in similar yields.

Synthesis of *o*-(methylthio)benzyl triphenylsilane (1)

To a suspension of Li metal (0.55 g, 79 mmol) in THF (20 mL) was added dropwise a solution of Ph_3SiCl (1.7 g, 5.8 mmol) in THF (15 mL) at 0 °C. The reaction mixture was allowed to warm to room temperature and stirred for 16 h resulting in a dark brown-black color. The solution was transferred via cannula to a dropping funnel and then added dropwise at –78 °C to a solution of *o*-(methylthio)benzyl chloride (*o*-(SCH₃C₆H₄)CH₂Cl, 1.0 g, 5.8 mmol) in THF (20 mL). This mixture was allowed to warm to room temperature and stirred for 16 h. The solvent was removed under reduced pressure, and the product was extracted with a solution of 80 mL of hexanes and 5 mL dichloromethane and subsequently filtered to remove LiCl. The crude material was recrystallized from a hot hexanes:dichloromethane solution (10:1).

o-(SCH₃C₆H₄)CH₂SiPh₃ (1) yield: 0.79 g (35%); mp 110–112 °C. ^1H NMR (CDCl_3) δ : 2.1 (3H, s, S-CH₃), 3.2 (2H, s, CH₂-Si), 7.5–6.9 (19H, m, Ph). ^{13}C NMR (CDCl_3) δ : 16.6 (S-CH₃), 21.2 (CH₂-Si), 125.1, 125.4, 127.3, 127.6, 129.0, 129.4, 134.4 (C_{ipso}), 135.9, 137.1 (C_{ipso}), 137.8 (C_{ipso}). ^{29}Si NMR (CDCl_3) δ : –11.9. Anal. calcd. for C₂₆H₂₄SSi: C 78.74, H 6.10; found: C 77.86, H 6.08.

o-(SCH₃C₆H₄)CH₂GePh₃ (2) yield: 0.93 g (37%); mp 104 °C. ^1H NMR (CDCl_3) δ : 2.1 (3H, s, S-CH₃), 3.2 (2H, s, CH₂-Ge), 7.7–6.9 (19H, m, Ph). ^{13}C NMR (CDCl_3) δ : 16.2 (S-CH₃), 22.2 (CH₂-Ge), 125.1, 125.4, 126.9, 127.9, 128.5, 128.8, 134.4 (C_{ipso}), 135.1, 136.6 (C_{ipso}), 138.2 (C_{ipso}). Anal. calcd. for C₂₆H₂₄GeS: C 70.79, H 5.48; found: C 70.01, H 5.46.

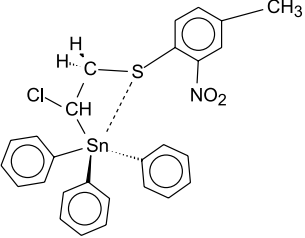
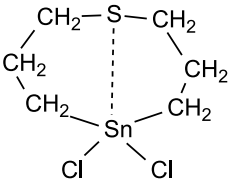
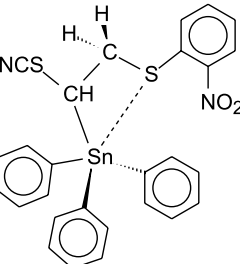
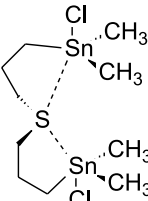
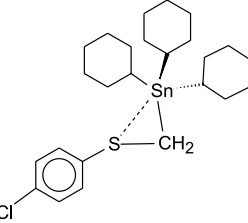
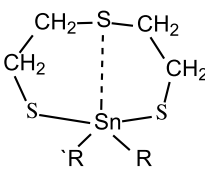
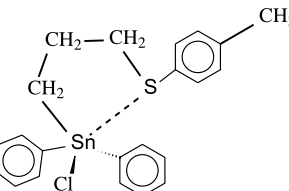
o-(SCH₃C₆H₄)CH₂SnPh₃ (3) yield: 2.0 g (71%); mp 106–108 °C. ^1H NMR (CDCl_3) δ : 2.1 (3H, s, S-CH₃), 3.1 (2H, s, CH₂-Sn, $J_{\text{H-}^{117}\text{Sn}} = 64.3$ Hz, $J_{\text{H-}^{119}\text{Sn}} = 66.7$ Hz), 7.6–7.0 (19H, m, Ph). ^{13}C NMR (CDCl_3) δ : 15.4 (S-CH₃), 20.5 (CH₂-Sn), 124.8, 125.0, 125.5, 127.6, 128.1 (Ph-Sn, $J_{\text{C-}^{117/119}\text{Sn}} = 180$ Hz), 128.6 (Ph-Sn, $J_{\text{C-}^{117/119}\text{Sn}} = 75$ Hz), 135.3 (C_{ipso}), 136.8 (Ph-Sn, $J_{\text{C-}^{117/119}\text{Sn}} = 150$ Hz), 139.1 (C_{ipso}), 139.2 (C_{ipso}). ^{119}Sn NMR (CDCl_3) δ : –115.5. Anal. calcd. for C₂₆H₂₄SSn: C 64.09, H 4.96; found: C 64.00, H 5.10.

o-(SCH₃C₆H₄)CH₂PbPh₃ (4) yield: 0.93 g (30%); mp 110–114 °C. ^1H NMR (CDCl_3) δ : 2.1 (3H, s, S-CH₃), 3.4 (2H, s, CH₂-Pb, $J_{\text{H-Pb}} = 75.53$ Hz), 7.6–6.9 (19H, m, Ph). ^{13}C NMR (CDCl_3) δ : 15.4 (S-CH₃), 31.3 (CH₂-Pb, $J_{\text{C-Pb}} = 286.8$ Hz), 124.7, 124.9, 125.1, 127.9, 128.1 (Ph-Pb, $J_{\text{C-Pb}} = 17.6$ Hz), 129.0 (Ph-Pb, $J_{\text{C-Pb}} = 72.6$ Hz), 135.4 (C_{ipso}), 137.2 (Ph-Pb, $J_{\text{C-Pb}} = 64.1$ Hz), 139.7 (C_{ipso}), 152.2 (Ph-Pb, $J_{\text{C-Pb}} = 359.2$ Hz). ^{207}Pb NMR (CDCl_3) δ : –146.2. Anal. calcd. for C₂₆H₂₄PbS: C 54.24, H 4.20; found: C 53.88, H 4.44.

Alternative synthesis of *o*-(methylthio)benzyl triphenyllead (4)

o-(Methylthio)benzyl chloride (1.0 g, 5.9 mmol) was added dropwise to a mixture of Ph_3PbCl (2.8 g, 5.9 mmol) and Mg turnings (0.15 g, 6.2 mmol) in THF (10 mL) at 0 °C. The reaction mixture was kept at 0 °C and allowed to stir until all the Mg had been consumed (16 h). The solution was transferred via cannula to another flask where the solvent was removed under reduced pressure and the product was extracted with 80 mL hexanes and 5 mL of dichloromethane and the solution filtered. The crude material was

Fig. 2. Summary of intramolecular interactions between tin and sulfur.

Structure	S—Sn (Å)	Reference	Structure	S—Sn (Å)	Reference
	3.67	7b		2.851	8a
	3.58	7b		3.097, 3.118	8b
	3.29, 3.26 ^a	7a		^a R=Cl R=Me: 2.863 ^a R=Br R=Me: 2.760, 2.767, 2.779, 3.514	9
	3.195	7c			

^a Two independent molecules in the unit cell.

recrystallized from a hexane:dichloromethane solution (10:1) and cooled to -20°C to yield **4**, 1.2 g (70%). This method was also used for the synthesis of **3** in a similar yield.

X-ray structural analysis

Crystals suitable for X-ray diffraction were obtained for compounds **1–4**, and **5** from hexane–dichloromethane solutions. Five colorless crystals **1**, **2**, **3**, **4**, and **5** were mounted

on glass fibers in a random orientation. Intensity data were collected at room temperature for **1**, **2**, **5** and -85°C for **3** using a Siemens/Bruker four-circle diffractometer with graphite-monochromated Mo $K\alpha$ radiation. Unit cell parameters and standard deviations were obtained by least-squares fit of 25 reflections randomly distributed in reciprocal space in the 2θ range of 15° – 30° . The ω -scan technique was used for intensity measurements in all cases. A range of 1.2° in ω and variable speed of 4.00–20.00 $^{\circ}/\text{min}$ was used for com-

pounds **1**, **2**, **3**, and **5**. Background counts were taken with a stationary crystal and total background time to scan time ratio of 0.5. Three standard reflections were monitored in all cases every 97 reflections and showed no significant decay. The data were corrected for Lorentz and polarization effects and a semiempirical absorption correction was also applied to the data set of **2** giving a min/max transmission ratio of 0.090:0.153. No absorption correction was applied to the data sets of **1**, **3**, and **5**.

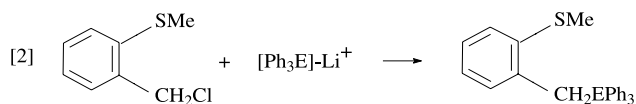
Intensity data for compound **4** were collected at room temperature on a Bruker SMART system with an APEX CCD detector. All structures were solved by direct methods and refined using the PC version of the SHELEXTL PLUS crystallographic software by Siemens.³ Full-matrix least-squares refinement of F^2 against all reflections was carried out with anisotropic thermal parameters for non-hydrogen atoms. Hydrogen atoms for **1**, **2**, **3**, and **5** were placed at calculated positions ($C-H = 0.96 \text{ \AA}$; $U_H = 0.08$) during refinements, whereas those in compound **4** were located on a difference map. The weighing scheme has the form $w^{-1} = \sigma^2(F_o^2) + (aP)^2 + bP$, where P is $[2F_c^2 + \max(F_o^2, 0)]/3$ and the final R factors have the form $R_1 = \sum |F_o - F_c| / \sum F_o$ and $R_w2 = \{\sum [w(F_o^2 - F_c^2)^2] / \sum [w(F_o^2)^2]\}^{1/2}$; these and some other relevant crystallographic parameters are summarized in Table 1 and selected bond lengths and angles are presented in Tables 2 and 3.

Compounds **1–3** (Figs. 3–5, respectively) crystallize in the triclinic form with space group $P-1$. The latter compound has two independent molecules in the asymmetric unit (**3a** and **3b**). Compound **4**, in contrast, crystallized in the monoclinic crystal structure with a space group of $P2(1)/c$ (Fig. 6).

Results and discussion

Synthesis and characterization

We have used two salt-elimination reactions to attach the *o*-(methylthio)benzyl chloride ligand to the group 14 atom (eqs. [1] and [2]).



Both routes are successful; however, when using the Grignard route we observed the significant production of the coupling product ($[\text{CH}_2(o\text{-C}_6\text{H}_4\text{SMe})]_2$ (**5**)). This is formed during the initial attempts to make the Grignard reagent prior to subsequent addition of the group 14 halide. Modification of the procedure to form the Grignard in situ in the

Fig. 3. Molecular diagram of **1**.

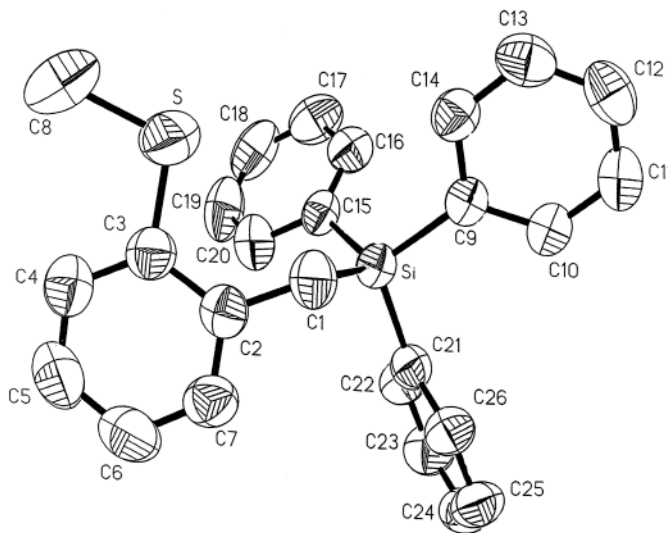
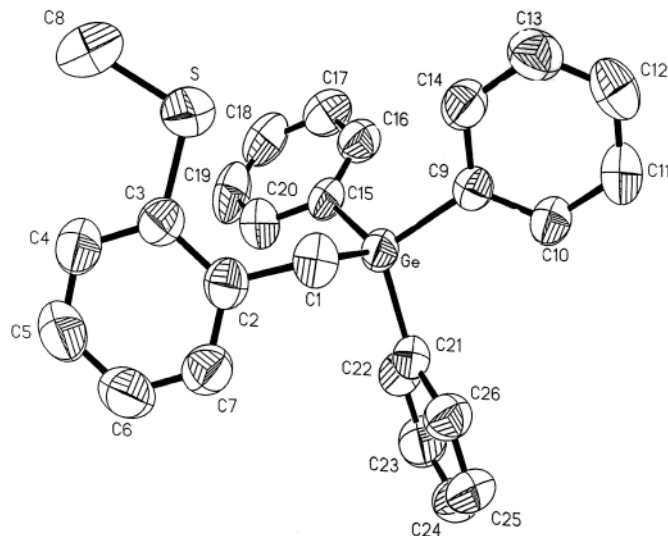


Fig. 4. Molecular diagram of **2**.



presence of the halide reduced the extent of this problem and resulted in the desired product in good yields (75%).

The reaction pathway involving the use of organometallic lithium salt was equally successful. However, we think the greater flexibility of the chemistry in eq. [1] makes this a more general and useful route to such compounds, where the organometallic lithium salts are less readily available. The spectroscopic and elemental analytical data for the compounds **1–4** are in total accord with their proposed structures, as is the data for **5**.

Periodic trends in the structural data for compounds **1–4**

The E-S intramolecular distance in compounds **1–4** is an essential structural feature for analysis of the progressive change E = Si, Ge, Sn, and Pb. Not only is it an indirect

³Supplementary data may be purchased from the Directory of Unpublished Data, Document Delivery, CISTI, National Research Council Canada, Ottawa, ON K1A 0S2, Canada (http://www.nrc.ca/cisti/irm/unpub_e.shtml for information on ordering electronically). CCDC 205424–205428 contain the crystallographic data for this manuscript. These data can be obtained, free of charge, via www.ccdc.cam.ac.uk/conts/retrieving.html (or from the Cambridge Crystallographic Data Centre, 12 Union Road, Cambridge CB2 1EZ, U.K.; fax +44 1223 336033; or deposit@ccdc.cam.ac.uk).

Table 1. Crystal data and structure refinement for crystal structure analysis of compounds 1–5.

	1	2	3	4	5
Empirical formula	C ₂₆ H ₂₄ SSi	C ₂₆ H ₂₄ SGe	C ₂₆ H ₂₄ SSn	C ₂₆ H ₂₄ SPb	C ₁₆ H ₁₈ S ₂
Formula weight (g/mol)	396.60	441.10	487.20	575.70	274.42
Temperature (K)	296(2)	296(2)	188(2)	296(2)	296(2)
λ (Mo K α) (Å)	0.71073	0.71073	0.71073	0.71073	0.71073
Crystal system	Triclinic	Triclinic	Triclinic	Monoclinic	Monoclinic
Space group	<i>P</i> -1	<i>P</i> -1	<i>P</i> -1	<i>P</i> 2(1)/ <i>c</i>	<i>P</i> 2(1)/ <i>n</i>
<i>a</i> (Å)	7.695(4)	7.704(3)	9.389(2)	19.139(3)	7.985(4)
<i>b</i> (Å)	7.746(5)	7.771(3)	11.440(4)	14.844(2)	4.866(2)
<i>c</i> (Å)	19.003(10)	19.195(6)	22.049(5)	7.8017(12)	18.875(6)
α (°)	98.42(5)	96.57(3)	77.94(2)	90	90
β (°)	95.76(4)	98.06(3)	78.36(2)	98.658(3)	92.79(3)
γ (°)	101.33(5)	102.14(3)	80.94(2)	90	90
Volume (Å ³)	1088.9(11)	1100.0(7)	2251.9(11)	2191.2(6)	732.5(5)
<i>Z</i>	2	2	4	4	4
<i>D</i> _X (Mg/m ³)	1.210	1.332	1.437	1.745	1.244
μ (mm ⁻¹)	0.212	1.496	1.236	7.803	0.344
<i>F</i> (000)	420	456	984	1112	292
Crystal size (mm)	0.80 × 0.52 × 0.20	0.80 × 0.72 × 0.28	0.40 × 0.18 × 0.14	0.12 × 0.08 × 0.06	0.30 × 0.24 × 1.16
θ Range for data collection (°)	2.19–25.05	2.17–25.05	1.83–24.94	2.55–28.28	2.16–25.05
Index ranges	0 ≤ <i>h</i> ≤ 9, –9 ≤ <i>k</i> ≤ 9, –22 ≤ <i>l</i> ≤ 22	0 ≤ <i>h</i> ≤ 9, –9 ≤ <i>k</i> ≤ 9, –22 ≤ <i>l</i> ≤ 22	–3 ≤ <i>h</i> ≤ 11, –13 ≤ <i>k</i> ≤ 13, –25 ≤ <i>l</i> ≤ 25	–25 ≤ <i>h</i> ≤ 25, –19 ≤ <i>k</i> ≤ 19, –10 ≤ <i>l</i> ≤ 10	–0 ≤ <i>h</i> ≤ 9, –0 ≤ <i>k</i> ≤ 5, –22 ≤ <i>l</i> ≤ 22
Reflections collected	4172	4190	10 790	29 981	2782
Independent reflections	3857	3876	7643	5446	1294
<i>R</i> (int)	0.0415	0.0491	0.0653	0.0473	0.0710
Absorption correction	N/A	Semi-empirical	N/A	SADABS	N/A
Refinement method	L.S. on <i>F</i> ²	L.S. on <i>F</i> ²	L.S. on <i>F</i> ²	L.S. on <i>F</i> ²	L.S. on <i>F</i> ²
Data/restraints/ parameters	3857/0/253	3857/0/253	7643/0/507	5446/0/254	1294/0/82
Goodness-of-fit on <i>F</i> ²	0.936	1.029	1.327	1.034	0.925
Final <i>R</i> indices (<i>I</i> > 2 σ (<i>I</i>))	<i>R</i> 1 = 0.0490, <i>wR</i> 2 = 0.1553	<i>R</i> 1 = 0.0581, <i>wR</i> 2 = 0.1705	<i>R</i> 1 = 0.0692, <i>wR</i> 2 = 0.1752	<i>R</i> 1 = 0.0350, <i>wR</i> 2 = 0.0770	<i>R</i> 1 = 0.0566, <i>wR</i> 2 = 0.1321
<i>R</i> indices (all data)	<i>R</i> 1 = 0.0668, <i>wR</i> 2 = 0.1753	<i>R</i> 1 = 0.0641, <i>wR</i> 2 = 0.1782	<i>R</i> 1 = 0.0861, <i>wR</i> 2 = 0.2247	<i>R</i> 1 = 0.0500, <i>wR</i> 2 = 0.0828	<i>R</i> 1 = 0.1371, <i>wR</i> 2 = 0.1688
Largest diff. peak, hole (e Å ⁻³)	0.255, –0.286	0.951, –1.147	1.425, –2.681	1.486, –0.696	0.129, –0.157

Table 2. Selected interatomic bond distances (Å) and angles (°) for the compounds **1–4**.

	E = Si (1)	E = Ge (2)	E = Sn a (3)	E = Sn b (3)	E = Pb (4)
Bond distances (Å)					
S—E	3.985	3.974	3.699	3.829	3.953
S—C(3)	1.753(3)	1.766(5)	1.766(11)	1.777(10)	1.754(5)
S—C(8)	1.776(4)	1.786(6)	1.812(12)	1.798(13)	1.786(6)
E—C(1)	1.896(3)	1.976(5)	2.174(8)	2.174(11)	2.244(5)
E—C(9)	1.873(3)	1.945(4)	2.143(9)	2.163(10)	2.204(5)
E—C(15)	1.876(3)	1.957(4)	2.145(9)	2.170(11)	2.192(5)
E—C(21)	1.876(3)	1.961(4)	2.156(9)	2.123(11)	2.200(5)
C(1)—C(2)	1.497(4)	1.491(6)	1.522(12)	1.462(15)	1.479(7)
Bond angles (°)					
C(9)–E–C(1)	104.57(12)	104.84(18)	112.6(4)	109.9(4)	103.35(18)
C(9)–E–C(15)	110.07(12)	110.17(17)	108.3(3)	109.0(4)	110.50(18)
C(9)–E–C(21)	109.87(11)	110.40(17)	108.0(3)	106.9(4)	109.21(18)
C(15)–E–C(1)	114.57(12)	115.20(19)	106.0(4)	110.1(5)	114.0(2)
C(15)–E–C(21)	107.48(11)	107.12(17)	109.0(3)	112.0(4)	107.00(19)
C(21)–E–C(1)	110.24(13)	109.1(2)	112.8(3)	108.9(4)	112.71(18)
C(2)–C(1)–E	118.27(19)	116.2(3)	112.2(6)	111.5(7)	114.1(3)
C(2)–C(3)–S	117.1(2)	116.7(3)	118.2(7)	117.6(8)	117.4(4)
C(4)–C(3)–S	123.1(2)	123.6(4)	122.6(9)	122.0(9)	123.1(4)
C(3)–S–C(8)	104.99(18)	107.7(3)	102.7(6)	102.7(6)	103.3(3)
C(10)–C(9)–E	123.40(19)	122.4(3)	118.8(7)	122.1(8)	119.7(4)
C(14)–C(9)–E	119.94(19)	119.6(3)	124.1(7)	122.6(7)	121.7(4)
C(16)–C(15)–E	121.17(19)	120.0(3)	121.5(7)	120.0(8)	122.0(4)
C(20)–C(15)–E	121.7(2)	122.0(3)	122.3(8)	121.4(9)	119.5(4)
C(22)–C(21)–E	121.81(19)	120.8(3)	118.6(7)	119.6(9)	121.4(4)
C(26)–C(21)–E	121.2(2)	120.9(3)	123.6(7)	120.9(9)	120.0(4)
C(1)–C(2)–C(3)	122.1(2)	122.5(4)	120.1(9)	121.2(10)	121.9(4)

Table 3. Selected interatomic bond distances (Å) and angles (°) for compound **5**.

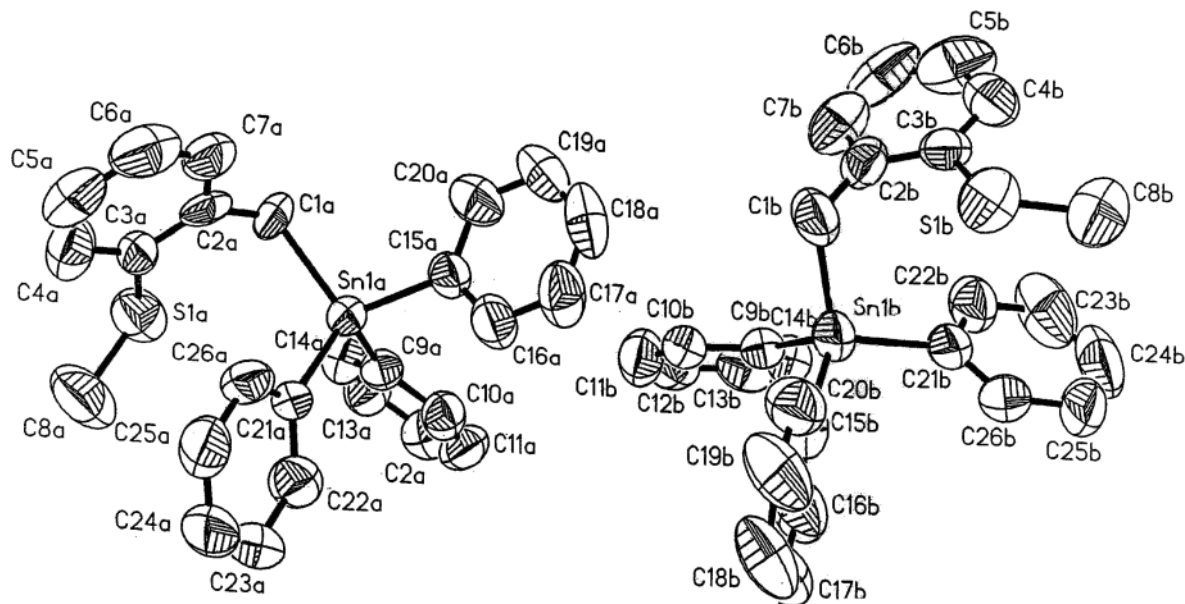
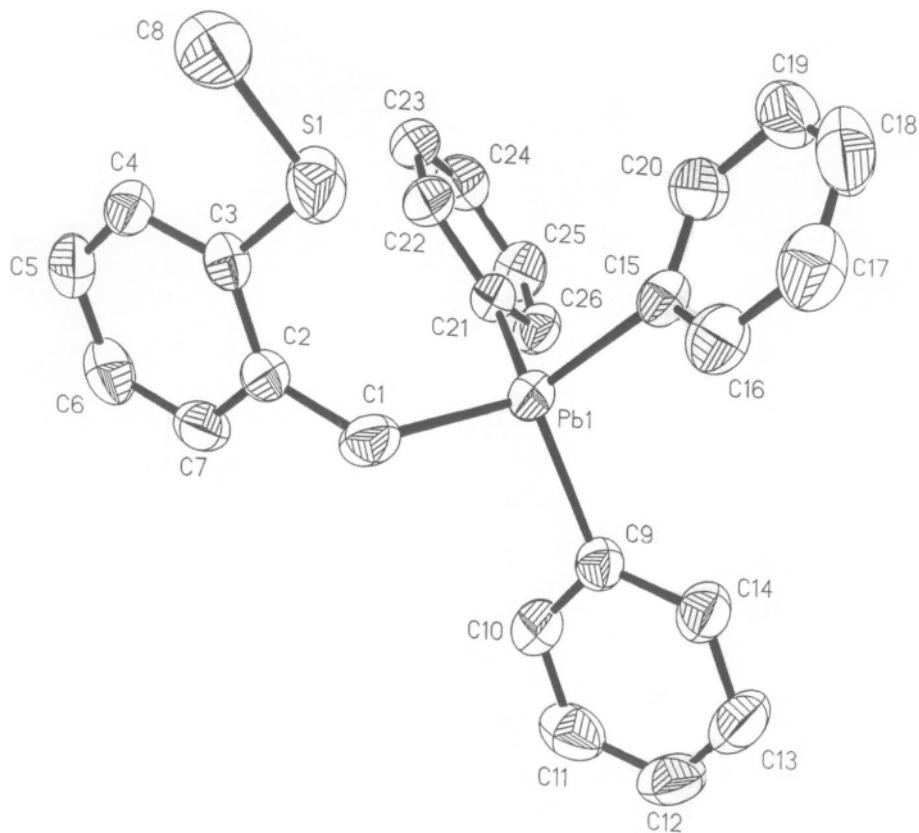
	5
Bond distances (Å)	
S—C(1)	1.768(4)
S—C(8)	1.770(5)
C(6)—C(7)	1.510(5)
Bond angles (°)	
C(6)–C(1)–S	117.9(3)
C(2)–C(1)–S	122.5(3)
C(1)–S–C(8)	104.9(2)
C(1)–C(6)–C(7)	121.9(4)
C(6)–C(7)–C(7a)	112.3(4)

method of testing the Lewis acidity toward S of the central metal atom, but it also lends a conformational degree of freedom that may effect any potential morphotropic transition. Table 4 is a summary of covalent radii (13), van der Waals (vdW) radii (13, 14), their sums, and their comparison to experimental E–S distances. Both **1** and **2** exhibit E–S distances that are ~100% of the sum of the vdW radii indicating that there are no significant intramolecular interactions between the metal center and sulfur. The Sn–S interactions in compound **3** are 3.699 Å (**3a**) and 3.829 Å (**3b**), an average distance of ~90% of the sum of the vdW radii, similar to that in the lead compound **4**, Pb–S = 3.953 Å, 91% of the vdW radii.

Both the ipso phenyl C—E bond lengths in compounds **1–4** vary as expected because of the greater atomic radius of the group 14 elements in the order Si < Ge < Sn < Pb and are similar to those reported in the series Ph₄E (**2–5**). Bonds between E and benzyl groups are not well represented in the literature, with the exception of that in Ph₃PbCH₂C₆H₅ (**15**). The present examples also exhibit the expected increase in bond lengths from C—Si to C—Pb, C1—E (E = Si, Ge, Sn, Pb) = 1.896, 1.976, 2.174, and 2.244 Å, respectively.

Consequences of E–S interaction on tetrahedral geometry

In a perfect tetrahedral geometry, each angle is 109.5° and the sum of three threefold symmetry angles will equal 328.5°. Group 14 organometallic compounds do not necessarily exhibit perfect tetrahedral geometry and the amount of distortion varies from system to system. In the Ph₄E system, all the molecules are spherical, crystallizing in the tetragonal space group *P* 42₁*c* (**2–5**). Despite the spherical nature and symmetry of these molecules, the C–E–C dihedral angles have a range of 108.1–111.2 (**2–5**). The wide range of angles creates difficulty when comparing systems; as a result, all angles of compounds **1–4** are compared with perfect tetrahedral geometry. The “base” of the tetrahedral in this series is comprised of the bond angles that would be *pushed* up as the sulfur atom approaches the metal center trans to the “axial” phenyl group. The numbering schemes for compounds **1** and **2** are identical; however, the numbering is slightly different in the phenyl region for **3** and **4**. For compounds **1** and **2**, angle C1–E–C9 is smaller than 109.5°, ranging from 104.57°

Fig. 5. Molecular diagram of **3**.**Fig. 6.** Molecular diagram of **4**.

for **1** to 104.84° for **2** with corresponding increases in C1-E-C15. As we would expect for compounds with no E-S interactions, the third angle (C9-E-C15) would also be close to 109.5° . The compounds **3a** and **4** (with E-S interactions of 88% and 91% of the sum of the vdW radii, respectively) have analogous angles that are smaller than 109.5° (108.0° and 107.0° , respectively). However, the other two angles in

the base do not adjust to preserve the sum of 328.5° , as in compounds **1** and **2**. When all three angles in the base plane are added together, **3a** and **4** have the largest differences from 328.5° , 333.4° , and 333.71° in that order, indicating that the C-E-C plane is being pushed up slightly by the E-S interactions. Table 5 summarizes the bond angles and their sums for compounds **1-4**.

Table 4. Comparison of sulfur – group 14 interactions.

E	Covalent radii (Å) ^a	van der Waals radii (Å) ^{a,b}	Σ_{Covalent} (Å)	$\Sigma_{\text{van der Waals}}$ (Å)	S—E (Å)	S—E as % vdW radii
Si	1.17	2.10	2.20	3.90	3.985	102.2
Ge	1.22	2.15	2.25	3.95	3.974	100.6
Sn	1.40	2.40	2.43	4.20	3.699 (a)	88.1
					3.829 (b)	91.2
					3.764 (avg.)	89.6
Pb	1.44	2.53	2.47	4.33	3.953	91.0
S	1.03	1.80				

^aSee ref. 13.^bSee ref. 14.**Table 5.** List of base and axial angles and their sums for compounds **1–4**.

Base angles	Sum of base angles (°)		Axial angles	Sum of axial angles (°)	
	1	2		1	2
C(15)-E-C(1)	329.21	330.21	C(9)-E-C(21)	327.59	326.62
C(9)-E-C(15)			C(1)-E-C(21)		
C(9)-E-C(1)			C(15)-E-C(21)		
	3a	3b		3a	3b
C(21)-E-C(1)	333.4	325.7	C(1)-E-C(15)	323.3	331.10
C(9)-E-C(21)			C(21)-E-C(15)		
C(9)-E-C(1)			C(9)-E-C(15)		
	4			4	
C(21)-E-C(1)	333.71		C(15)-E-C(9)	323.06	
C(15)-E-C(21)			C(1)-E-C(9)		
C(15)-E-C(1)			C(21)-E-C(9)		

Further indications of the distortion about the central metal atom are the axial angles. The sum of these angles under normal geometry would also be 328.5°. Once the base plane is pushed up by increasing E–S interactions, the sum of these three angles mentioned above should be *less than* 328.5°. Indeed after analysis, the two compounds with the smallest sums are **3a** (323.3°) and **4** (323.06°), precisely the compounds with the shortest E–S distances in terms of % Σ vdW radii.

Another trend that illustrates how the E–S interaction distorts the molecule is that as the E–S distance decreases, the C(2)–C(1)–E bond angle decreases as well. This makes sense because angle C(1)–C(2)–C(3) will not change much because of the rigid angle system dictated by the aromatic ring. As a result, the only angle within the “arm” substructure that gives flexibility is the C(2)–C(1)–E angle, which contains the methylene moiety. Shortening of the E–S distance would be facilitated by a contraction of the C(2)–C(1)–E angle. Indeed this angle does contract when comparing **1** and **2** with compounds **3** and **4**, with the minimum occurring at compound **3**.

Isostructural considerations

We have investigated the possible isostructural relationships of **1–4**. From their respective structural data **1** and **2** seem to be isostructural. However, due to the high degree of freedom of assigning a triclinic unit cell and putting the molecule in that cell with respect to the eight centers of symmetry, the observation is not truly a proof. We computed a least-squares fit of these two molecules including all non-

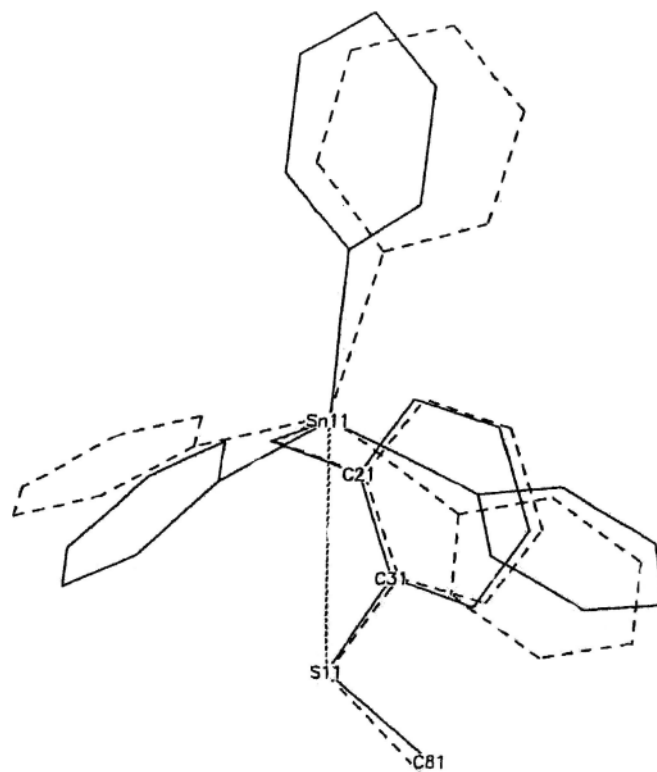
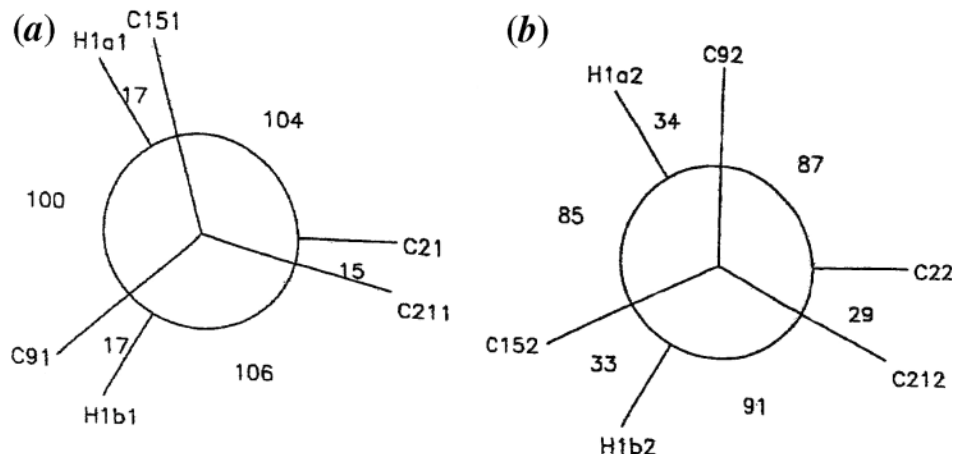
Fig. 7. Superposed structures of **3a** and **3b**.

Fig. 8. Solid-state conformational analysis of **3**. (a) View down Sn(1)–Ca(1), (b) view down Snb(1)–Cb(1).**Table 6.** Molecular volumes and packing coefficients for **1–4**.

Molecule	Volume (Å ³)	Packing coefficient
Si	371.1	0.68
Ge	374.6	0.68
Sn 1	386.1	0.69
Sn 2	385.9	0.69
Pb	388.3	0.71

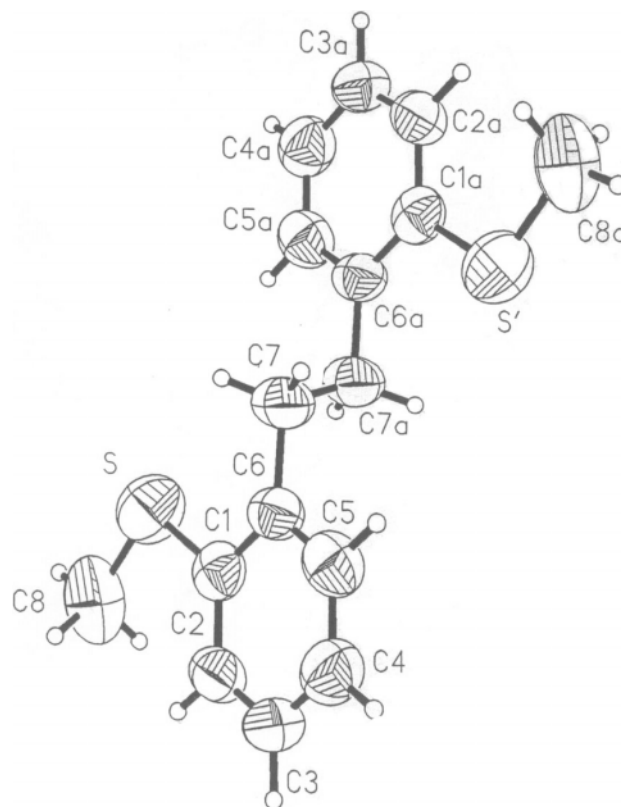
hydrogen atoms and the mean distance is 0.100 Å; RMS = 0.0823, a rather good fit. To prove absolutely we refined the Si structure with the coordinates of the Ge compound and in this manner proved that **1** and **2** are isostructural ($R = 0.0476$). The Sn and Pb derivatives do not belong (in the sense of isostructurality) to a homologous series.

A superpositioning of the two forms of the tin compound (**3a** and **3b**) is illustrated in Fig. 7 and their two distinct conformations are presented in Fig. 8. The two independent molecules are not superimposable, except to a high degree the Sn–S interaction grouping, despite their differing Sn–S distances. The two forms have fully staggered (**3b**) and partially eclipsed forms (**3a**), which is similar to other organometallic group 14 compounds (16). Thus, despite being relatively weak, the intramolecular Sn–S interactions have a significant effect upon the conformational character of the two molecules.

We have computed molecular volumes and packing coefficients for **1–4** (Table 6). These data illustrate a significant jump in the molecular volume between Ge and Sn, where the morphotropic step occurs. Overall, the packing coefficients are very similar, and the slight increase in the value for lead could be the driving force for the change in its crystal form.

Magnesium-induced dimerization of *o*-(SCH₃)C₆H₄CH₂Cl

The capacity of Grignard reagents to produce dimers of their parent organic halides is well established, thus the formation of **5** from such attempted reactions is not surprising. In 1980 an attempt by Zheltov et al. (17) to study the conjugation of aromatic disulfides by UV, mentions the preparation of compound **5**, however, studies were limited, hence we have performed a single crystal structural analysis.

Fig. 9. Molecular diagram of **5**.

Compound **5** (Fig. 9) crystallized in the monoclinic crystal group with a space group of $P2(1)/n$. In total its structure is unremarkable, however, the various bond lengths and angles about the S atom serve as a baseline to note any variations in **1–4** by virtue of the intramolecular E–S interactions (Table 5).

Acknowledgments

Support for this research was provided by the R.A. Welch Foundation, Houston, Texas (Grant AH-0546) and SCORE NIH (Grant No. S06-GM-08012). L.P. wishes to thank the Hungarian Academy of Sciences for the leave of absence.

References

1. A.I. Kitaigorodskii. Organic chemical crystallography, Consultants Bureau, New York. 1961. p. 223.
2. V. Gruhnert, A. Kirfel, G. Will, F. Wallrafen, and K. Recker. *Z. Kristallogr.* **163**, 53 (1983).
3. A. Karipides and D.A. Haller. *Acta Crystallogr.* **B28**, 2889 (1972).
4. V.K. Belsky, A.A. Simonenko, V.O. Reikhsfeld, and I.E. Saratov. *J. Organomet. Chem.* **244**, 125 (1983).
5. H. Preut and F. Huber. *Acta Crystallogr.* **C49**, 1372 (1993).
6. L. Párkányi, A. Kálmán, S. Sharma, D.M. Nolen, and K.H. Pannell. *Inorg. Chem.* **33**, 180 (1994).
7. (a) P.J. Cox, S.M.S.V. Doidge-Harrison, I.W. Nowell, R.A. Howie, R.P. Randall, and J.L. Wardell. *Inorg. Chim. Acta*, **172**, 225 (1990); (b) R.A. Howie, J.L. Wardell, E. Zanetti, P.J. Cox, and S.M.S.V. Doidge-Harrison. *J. Organomet. Chem.* **431**, 27 (1992); (c) P.J. Cox, S.M.S.V. Doidge-Harrison, I.W. Nowell, R.A. Howie, J.L. Wardell, and J.M. Wiggzell. *Acta Crystallogr.* **C46**, 1015 (1990).
8. (a) K. Jurkschat, J. Schiling, C. Mügge, and A. Tzschach. *Organometallics*, **7**, 38 (1988); (b) K. Jurkschat, B. Schmid, M. Dybiona, U. Baumeister, H. Hartung, and A. Tzschach. *Z. Anorg. Allg. Chem.* **560**, 110 (1988).
9. U. Kolb, M. Beuter, M. Gerner, and M. Dräger. *Organometallics*, **13**, 4413 (1994).
10. R. Grice and L.N. Owen. *J. Chem. Soc.* 1947 (1963).
11. A. Kucsma and T. Kremmer. *Acta Chim. Acad. Sci. Hung.* **34**, 71 (1962).
12. V.J. Traynelis and D.M. Borgnaes. *J. Org. Chem.* **37**, 3824 (1972).
13. J.E. Huheey, E.A. Keiter, and R.L. Keiter. *Inorganic chemistry: Principles of structures and reactivity*. 4th ed. Harper Collins College Publishers, New York. 1993. p. 292.
14. R. Chauvin. *J. Phys. Chem.* **96**, 9194 (1992).
15. U. Fahrenkamp, M. Schuermann, and F. Huber. *Acta Crystallogr.* **C50**, 1707 (1994).
16. (a) K.H. Pannell, L. Párkányi, H. Sharma, and F. Cervantes-Lee. *Inorg. Chem.* **31**, 522 (1992); (b) L. Párkányi, C. Hernandez, and K.H. Pannell. *J. Organomet. Chem.* **301**, 145 (1986); (c) K.H. Pannell, R.N. Kapoor, R. Raptis, L. Párkányi, and V. Fülöp. *J. Organomet. Chem.* **384**, 41 (1990); (d) L. Párkányi, and E. Hengge. *J. Organomet. Chem.* **235**, 273 (1982).
17. A.Ya. Zheltov, E.N. Avramenko, and B.I. Stepanov. *Zh. Org. Khim.* **16**, 384, (1980).